THE JOURNAL OF PHYSICAL CHEMISTRY B

Article

pubs.acs.org/JPCB

Biomimetic Dual Sensing-Actuators Based on Conducting Polymers. Galvanostatic Theoretical Model for Actuators Sensing Temperature

Toribio F. Otero,*[,†] Juan J. Sanchez,[†] and Jose G. Martinez[†]

[†]Universidad Politécnica de Cartagena, ETSII, Center for Electrochemistry and Intelligent Materials (CEMI), Paseo Alfonso XIII, Aulario II, 30203 Cartagena, Spain

Supporting Information

ABSTRACT: A theoretical model is proposed for the quantitative description of the chronopotentiometric (*E-t*) responses, under galvanostatic control, of either conducting polymer films or dual sensing-actuating devices. Assuming that the reaction occurs by extraction, or injection, of *n* consecutive electrons from, or to, a polymer chain the material moves through *n* consecutive oxidation or reduction states. Stair functions are obtained describing either potential or consumed electrical energy evolutions as a function of both, driving (current) and environmental (temperature, electrolyte concentration...) variables. The current quantifies the actuation of any electrochemical device (charge/discharge of batteries, movement rate, and position of muscles): the stair functions are dual actuating-sensing functions. A good agreement exists between theoretical and experimental results from either polypyrrole films or artificial muscles at different temperatures. Only two connecting wires include, at any time, sensing (potential) and working (current) information of any dual device.

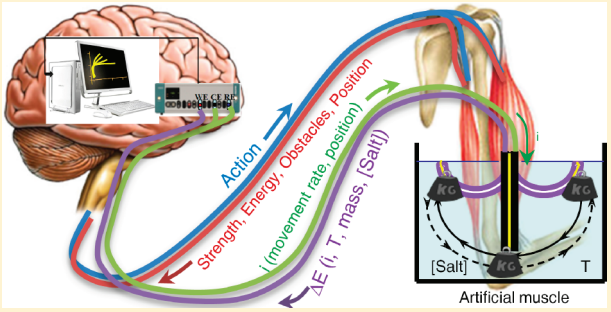

INTRODUCTION

Conducting polymers (CPs), when considered as reactive materials (they can be oxidized and reduced in a reversible way), provide electrochemical properties as electro-chemo-mechanical, electro-chromic, charge storage, electro-chemo-porosity, electron-ion transduction, and so on.[1,2] The material composition mimics that of natural organs: reactive macromolecules, solvent, and ions. Based on those reactive properties, reactive biomimetic devices and products such as artificial muscles,[3−11] smart windows,[12−15] smart membranes[16−21] or batteries and supercapacitors,[22−25] smart chemical dosage;[26,27] electron/ion transduction at very low overpotential and nervous[28,29] interfaces; wettability[30−32] and so on are being developed. Most of those devices may act, while working (moving, changing its color, etc.), as sensors of the surrounding conditions. Artificial muscles sensing working temperature,[33,34] electrolyte concentration,[33,35] or attached and shifted weights,[35] and tactile muscles sensing obstacles[4] and indicating the mechanical resistance of the obstacle to be shifted have been developed. Three layer artificial muscles also can be considered as mobile batteries (charging during movement in one direction and discharging-a fraction of the working energy can be recovered- while moving in the opposite direction) sensing working conditions.[3,4,34−36] All those electrochemical devices constitute unique actuator/sensor systems only preceded by natural organs in mammals. When we touch and catch an object in darkness, our brain knows the exact energy that our muscles need to produce to move the obstacle. Muscles in arms are electro-chemo-mechanical motors that sense the mechanical energy required to shift the obstacle.

Mimetic sensing and tactile electrochemical artificial muscles are several (one actuator and several sensors: temperature, electrolyte concentration, obstacles) in one device working simultaneously. The actuator here is a soft electrical motor which movement rate and position are, under current and charge control, described by faradic equations.[3,11,37] The evolution of the device potential or that of the consumed electrical energy while working are the empirical sensing magnitudes.[4,33−35] At the moment this biomimetic, dual and simultaneous actuating-sensing property is outside any theoretical description.

The above-described electrochemical (reactive) devices, developed from conducting polymers, can work under flow of constant currents. The material adjusts its potential to the oxidation state attained at every oxidation time by the polymer film giving a chronopotentiometric response (Figure 1). The continuous linear increase of the potential with time used to be considered as evidence of the capacitive nature of electrochemical responses from conducting polymers.[38−47] For redox processes, like batteries, one or several plateaus should be expected at increasing potentials. An unexpected result for a capacitor is that, after consumption of a constant charge, the potential steps to very high values (Figure 1), like in batteries at the end of the charge process.

Received: January 10, 2012
Revised: March 23, 2012
Published: March 28, 2012

   dx.doi.org/10.1021/jp300290s | *J. Phys. Chem. B* 2012, 116, 5279−5290

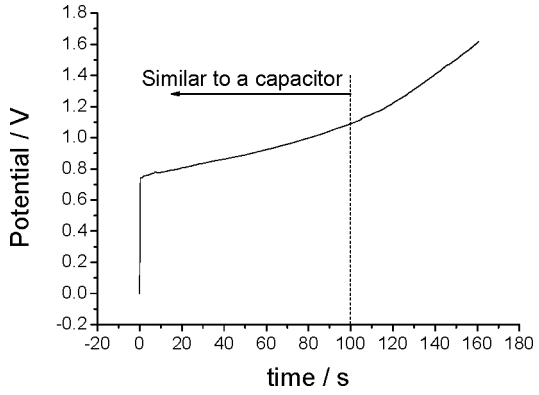

Figure 1. Experimental chronopotentiogram obtained from a free-standing polypyrrole film weighing 1.7 mg and having 1 cm^2 of the film in 0.1 M $LiClO_4$ aqueous solution at room temperature by flow of 0.4 mA.

Theoretical approaches to redox processes in CPs do not present a generally accepted model. Several attempts exist for the description of voltammetric responses to cyclic potential sweeps[48−53] or for chronoamperometric responses to potential steps.[54−59] Chronopotentiometric responses have been modeled from impedance results using equivalent electrical circuits.[60,61] As far as we know, only Micka et al.[62] tried to propose a self-supporting model (without adjustable parameters) for polyacetylene oxidation based on the empirical dependence of the electrical conductivity and the stationary potential on the degree of doping, not considering experimental chemical variables. The evolution of the potential at open circuit was studied by Pernaut et al. employing pulse chronopotentiometric experiments and concepts from diffusion.[63]

In this paper we propose an initial physicochemical approach to the description of the actuating-sensing properties of conducting polymers, materials, and devices, working under galvanostatic control. Theoretical and experimental results will be presented for self-supported polypyrrole responses at different temperatures and compared with those existing for artificial muscles sensing temperature (the actuator, an artificial muscle, sense ambient temperature) while working.[33,34]

EXPERIMENTAL METHODS

Simulations have been performed using MATLAB 7.7.0.0471 (R 2008b) software.

Pyrrole (Fluka) was purified by distillation under vacuum using a diaphragm vacuum pump MZ 2C SCHOTT and stored under nitrogen atmosphere at −10 °C. Anhydrous lithium perchlorate salt (Fluka) and acetonitrile (Panreac, HPLC grade) were used as received.

Polypyrrole films were electrogenerated from 0.2 M pyrrole and 0.1 M $LiClO_4$ acetonitrile solution including 2% of water content in order to avoid parallel chemical polymerization.[64] The working electrode was an AISI 304 stainless steel plate (the low adherence of the generated polymer allows to remove quite thin films from it to get self-supported electrodes or films for the construction of different devices) having 4 cm^2 of surface area. As counter electrodes two similar stainless steel electrodes were used, one by side of the working electrode and at the same distance (0.5 cm) in order to get a uniform electric field. A Metrohm Ag/AgCl (3 M KCl) electrode was used as reference electrode. Potentials in this work are referenced to it.

Polypyrrole was electrogenerated by consecutive square potential waves between −0.322 V (kept for 2 s) and 0.872 V (kept for 8 s) in order to control the film morphology and adherence.[64] The overall polymerization charge (anodic minus cathodic charges) was 28 C. After reduction at −0.322 V for 300 s two dry films, one by electrode side, were peeled off from the electrode and weighted in a Sartorious SC2 balance having a precision of 10^{-7} g. Average film thicknesses of 13 μm were measured using an electronic micrometer having a precision of 1 μm. Those films were cut in different strips, weighed, and used as self-supported polypyrrole electrodes in the background electrolyte. The direct contact between the electrolyte and the metallic clamp by capillarity through the polypyrrole film (self-supported or taking part of artificial muscles) was avoided by two transversal paint strips 1 mm below the electrode top. The electrolyte meniscus touched the lower paint strep. The mass of the immersed polypyrrole film (1.6026 mg) was calculated by extrapolation from the immersed film area (Figure 2).

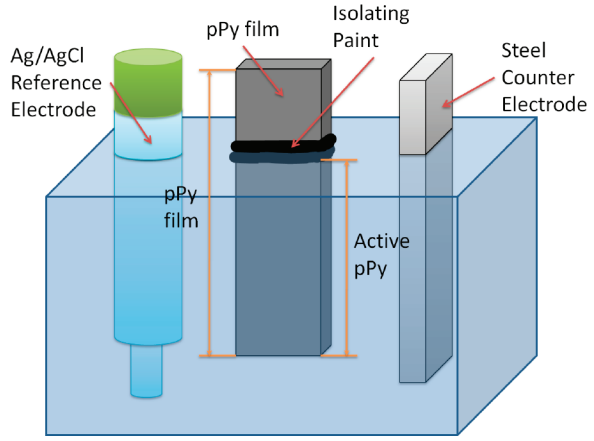

Figure 2. Experimental setup employed during experiments.

All the electrochemical experiments were performed using a potentiostat-galvanostat Autolab PGSTAT100. Ultrapure water was obtained from a Milli-Q equipment. The cell temperature was maintained constant by means of a Julabo F25 cryostat (±0.1 °C) while studying the effect of the temperature. The experimental chronoamperometric results were obtained by submitting self-supported polypyrrole films to consecutive square waves, ±0.75 mA, of 200 s (0.75 mA flow for 100 s, −0.75 mA flow for 100 s) in the background electrolyte until stationary responses (3−4 cycles). The stationary anodic and cathodic responses will be considered here.

MODEL DEVELOPMENT

Oxidation/reduction reactions in a film of conducting polymer (self-supported or taking part of any electrochemical device) exchanging anions with the electrolyte during reactions used to be summarized as

$$(Pol^*)_s + n(A^-)_{sol} + m(S) \underset{red}{\overset{ox}{\rightleftarrows}} [(Pol)^{n+}(A^-)_n(E)_m]_{gel} + ne^- \quad (1)$$

where the different subindexes mean the following: s, solid; sol, solution; Pol^* represents the active centers on the neutral polymer chains, understood as those points on the polymeric chains where a positive charge will be present after oxidation; A^- represents the anions exchanged with the electrolyte in order to keep the electroneutrality inside the material; S represents solvent

dx.doi.org/10.1021/jp300290s | J. Phys. Chem. B 2012, 116, 5279−5290

molecules exchanged for osmotic pressure balance forming a dense polymer gel (indicated by the sub index gel); and n represents either the number of electrons removed from the polymeric chains during oxidation (injected during reduction) or the number of anions penetrating from solution for charge balance.

Complex electrochemical reactions like reaction 1 involving two or more reactants during electron transfer and having reaction orders other than 1 have been treated by Prof K. J. Veter.[65] The oxidation empirical reaction rate from reaction 1 under flow of constant anodic currents (i_a) is

$$r = \frac{i_a}{FV} = k_a[A^-]^d[Pol^*]^e \tag{2.a}$$

where r represents the polymer oxidation rate; k_a is the oxidation rate constant, or the rate coefficient, the subindex a indicates anodic process; superscripts d and e are the reaction orders; $[A^-]$ is the concentration of anions in solution, and $[Pol^*]$ is the concentration of active centers in the polymeric film; F is the Faraday constant (F = 96485 C mol^{-1}), and V is the volume of the polymeric film. In this initial approach we use concentrations instead of the most correct magnitude: activities.

For reduction reactions, the empirical kinetics from eq 1 will be

$$r = \frac{i_c}{FV} = k_c[(Pol)^{n+}(A^-)_n]^f \tag{2.b}$$

where k_c is the reduction rate constant, or rate coefficient, for the polymer reduction by flow of a cathodic current i_c, $[(Pol)^{n+}(A^-)_n]$ is the concentration of oxidized species in the film, and the superscript f is the reaction order.

Taking into account the potential dependence of the rate coefficients for anodic or cathodic reactions according with Butler–Volmer, the current (the reaction rate) passing through a polymeric film (self-supported or taking part of an electrochemical device) during a galvanostatic experiment becomes

$$i_a = FVk_a[A^-]^d[Pol^*]^e = FVk_{a0}[A^-]^d[Pol^*]^e \exp\left(\frac{(1-\alpha)nF(E-E_0)}{RT}\right) \tag{3.a}$$

$$i_c = FVk_c[(Pol)^{n+}(A^-)_n]^f = FVk_{c0}[(Pol)^{n+}(A^-)_n]^f \exp\left(\frac{\alpha nF(E-E_0)}{RT}\right) \tag{3.b}$$

where the subindex a indicates anodic process and c indicates cathodic process, E is the electrode potential, E_0 is the standard potential, α is the symmetry factor, k_0 is the pre-exponential factor, R is the universal gas constant (R = 8.314 J K^{-1} mol^{-1}), and T is the working temperature.

From here the evolution of the material potential (E_a or E_c), under flow of anodic or cathodic currents, can be obtained

$$E_a = E_0 + \frac{RT}{(1-\alpha)nF}\left(\ln\left(\frac{i_a}{FV}\right) - d\ln[A^-] - e\ln[Pol^*] - \ln k_{a0}\right) \tag{4.a}$$

$$E_c = E_0 + \frac{RT}{\alpha nF}\left(\ln\left(\frac{i_c}{FV}\right) - f\ln[(Pol)^{n+}(A^-)_n] - \ln k_{c0}\right) \tag{4.b}$$

Equations 4.a and 4.b indicate that the potential of the material is a function of the physical and chemical variables: the working temperature (T); the imposed current (i_a or i_c); the electrolyte concentration $[A^-]$; the concentration of active centers in the film $[Pol^*]$; and the mechanical or structural (chain conformations) conditions through V and k_{a0}.[48,49,55,66−68]

Those two equations contain the kinetics of the actuation, through i_a and i_c, of any device (movement and position of artificial muscles,[3,11,35,37] charge/discharge in batteries, absorbance variation rates in smart windows and so on), which actuation is based on the electrochemistry of CPs. Moreover, eqs 4.a and 4.b define the ability of the potential evolution in those devices to sense the following: working temperature,[33,34] electrolyte concentration,[33,35] or mechanical conditions[35] while working. Those equations provide a theoretical description of dual sensing and actuating electrochemical devices, including sensing and tactile artificial muscles.[36]

Equation 4 includes, implicit, the time of current flow. As stated above, the concentration of active centers in the film ($[Pol^*]$) is related to those points of the polymeric chains that will store positive charges in the polymeric chains at the end of the oxidation process. Thus, the evolution of the concentration of active centers in the film volume with time decreases, under current flow, following the consumed charge[64]

$$[Pol^*] = [Pol^*]_{initial} - [Pol^*]_{consumed} = [Pol^*]_{initial} - \frac{Q}{FV} = [Pol^*]_{initial} - \frac{it}{FV} \tag{5.a}$$

where $[Pol^*]_{initial}$ is the initial concentration of active centers, $[Pol^*]_{consumed}$ is the concentration of active centers consumed during the oxidation time, and Q is the involved charge. Starting from the same initial concentration every time and passing the same charge (by imposing the same constant current flowing for the same time) the same final concentration of active centers will be attained every time. When a reduction reaction is studied, the concentration of active centers generated by flow of a constant cathodic current i_c during a time, t, is

$$[Pol^*] = \frac{it}{FV} \tag{5.b}$$

Self-supported films and devices of conducting polymers are studied in high salt concentrations, using electrolyte volumes large enough to accept that the salt concentration remains constant during oxidation/reduction reactions

$$[A^-] = [A^-]_{initial} \tag{6}$$

Under those conditions the influence of the diffusion of the ions through the electrolyte toward or from the surface of the polymer film is assumed to be negligible.

The diffusion of the counterions inside the dense gel film, from or toward the active centers, plays an important role during redox processes. Working under potentiostatic conditions the current, $i(t)$, required to oxidize the material (at any oxidation time, t, after a potential step) under diffusion kinetic control of the charge balance counterions inside the film was described by a stretched exponential function[68−70]

$$i(t) = bQ\exp(-bt) \tag{7}$$

dx.doi.org/10.1021/jp300290s | J. Phys. Chem. B 2012, 116, 5279−5290

where Q is the oxidation charge, the constant b includes D, the diffusion coefficient of the charge balance counterions across the partially oxidized material toward the chain active centers, and the film thickness, h

$$b = \frac{2D}{h^2} \tag{8}$$

Now, for galvanotatic experiments the current at any time equals the initial current at $t = 0$ s, and

$$i = bQ = \frac{2D}{h^2 Q} \tag{9}$$

By substitution of Q during the development of eq 5.a the diffusion coefficient and the film thickness can be included in the theoretical expression when required. Here we will go on the kinetic development based on the chemical kinetic control of the polymer reactions. As in every electrochemical process the imposed current defines the reaction rate: the counterion diffusion flow inside the film must adjust to this current (eq 9) to keep the charge balance in the film, reaction 1, at every time according to Faraday's laws; otherwise the resistance rises and the potential should evolve to meet a new reactive process. The oxidation process, in this context, occurs under chemical reaction kinetic control, and eq 9 only is required for the determination of the diffusion coefficient, if required.

Related to the film volume, variation percentages around 1% were estimated from independent dimensional determinations (length of self-supported films or width in films coating electrodes or glasses) measured by different experimental methodologies.[71−79] When larger initial variations (2−20%) were described[80−85] a stationary state, with volume variations around 1%, was recovered after a few potential sweeps. So, in this initial theoretical approach we can consider a constant film volume during oxidation or reduction. Actual volume variations will be recovered in a subsequent paper for the theoretical description of dual mechanical sensing electrochemical devices. On the other hand during electrochemomechanical characterizations of artificial muscles the incertitude related to volume variations has been avoided by using specific (per unit of reduced and dry polymer weight) concentrations (active centers or counterions), specific currents of specific charges.[3,11,34,37,86]

In this initial theoretical approach the polymer swells and shrinks during oxidation/reduction, respectively, reactions. Deep reduction states with conformational packing of the polymeric structure and subsequent conformational relaxation kinetic control of the oxidation reaction are avoided.

During reduction reactions, eq 4.b includes the concentration of the oxidized polymeric compound, $[(Pol)^{n+}(A^-)_n]$, in the film, which is related to the concentration of the reactants through the equilibrium constant (reaction 1)[87]

$$K = \frac{k_c}{k_a} = \frac{[(Pol)^{n+}(A^-)_n]^f}{[A^-]^d [Pol^*]^e} \tag{10}$$

And the concentration of the oxidized species becomes

$$[(Pol)^{n+}(A^-)_n]^f = \frac{k_c}{k_a}[A^-]^d [Pol^*]^e \tag{11}$$

Thus, from eqs 4, 5, and 11 a new expression is obtained for the evolution of the reactive material potential as a function of the time of current flow (chronopotentiogram) and different experimental variables: applied current, concentration of anions in solution, temperature, and concentration of active centers in the polymer film

$$E_a(t) = E_0 + \frac{RT}{(1-\alpha)nF}\left\{\ln\left(\frac{i_a}{FV}\right) - d\ln[A^-] - e\ln\left([Pol^*]_{initial} - \frac{i_a t}{FV}\right) - \ln k_{a0}\right\} \tag{12.a}$$

$$E_c(t) = E_0 + \frac{RT}{\alpha nF}\left\{\ln\left(\frac{i_c}{FV}\right) - \frac{k_c}{k_a}d\ln[A^-] - \frac{k_c}{k_a}e\ln\left(\frac{i_c t}{FV}\right) - \ln k_{c0}\right\} \tag{12.b}$$

Simulated chronopotentiograms from eq 12.a using a constant anodic current of 0.75 mA are presented in Figure 3

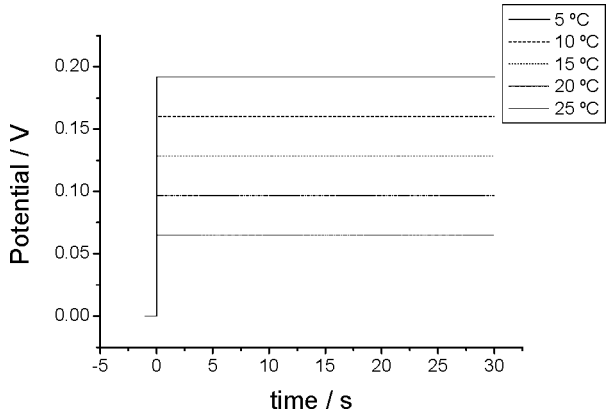

Figure 3. Simulation of eq 12.a using a constant anodic current (i_a) of 0.75 mA, for different temperatures (5, 10, 15, 20, and 25 °C); being the electrolyte concentration $[A^-]$ = 1 mol L^{-1}, and the initial concentration of active center, $[Pol^*]$ = 2 mol L^{-1}; assuming α = 0.5, and n = 1, for a polymeric film which *length* = 1 cm, *width* = 1 cm, *weight* = 1.6 mg, *density* = 1540 g L^{-1}.

for different temperatures (5, 10, 15, 20, and 25 °C); being the electrolyte concentration $[A^-]$ = 1 mol L^{-1}, and the initial concentration of active centers, $[Pol^*]$ = 2 mol L^{-1}; assuming α = 0.5, and n = 1, for a polymeric film which *length* = 1 cm, *width* = 1 cm, *weight* = 1.6 mg, *density* = 1540 g L^{-1}.

As expected from a reactive sensor (eq 12) the potential evolves at lower values for increasing temperatures. Nevertheless theoretical slopes (E-t) are very low (almost constant value) when compared with experimental results (Figure 1), those low slopes were expected for batteries based on one redox process.

In a second approach the polymer films can be considered as constituted by ideal polymeric chains having the same length (monodisperse polymer). Every chain loses n electrons under flow of a constant anodic current (galvanostatic experiment) through n consecutive oxidation steps of one electron per step. At the oxidation potential onset, E_1, the extraction of the first electron from every polymeric chain starts, reaching the first oxidation step.

For n = 1

$$(Pol)_s + (A^-)_{dis} \rightleftarrows Pol^+A^- + e^- = >E_1, E_{01} \tag{13.a}$$

where E_1 is the first equilibrium potential, and E_{01} is its standard potential.

dx.doi.org/10.1021/jp300290s | J. Phys. Chem. B 2012, 116, 5279−5290

When all the chains store a positive charge the potential steps to the value required to extract a second electron attaining a new oxidation state.

For $n = 2$

$$Pol^{+}A^{-} + (A^{-})_{dis} \rightleftarrows Pol^{2+}(A^{-})_2 + e^{-} => E_2, E_{02} \quad (13.b)$$

E_2 and E_{02} (equilibrium and standard potential) are more anodic potentials than E_1 and E_{01} ($E_2 > E_1$).

The oxidation goes on passing through n consecutive intermediate oxidation states each starting at increasing equilibrium potentials

$$E_1 < E_2 < E_3 < .... < E_{n-1} < E_n \quad (14)$$

being E_{01}, E_{02}, ..., E_{0n}, the standard potentials for the concomitant equilibriums. For the n^{th} oxidation step (extraction of the n^{th} electron from every chain)

$$Pol^{(n-1)+}(A^{-})_{n-1} + (A^{-})_{dis} \rightleftarrows Pol^{n+}(A^{-})_n + e^{-} => E_n, E_{0n} \quad (13.c)$$

Each equilibrium potential, E_1, E_2, ..., E_n, and concentrations there involved are linked by the Nernst equation

$$E_1 = E_{01} + \frac{RT}{F}\ln\frac{[Pol^{+}A^{-}]}{[Pol][A^{-}]} \quad (15.a)$$

$$E_2 = E_{02} + \frac{RT}{F}\ln\frac{[Pol^{2+}(A^{-})_2]}{[Pol^{+}A^{-}][A^{-}]} \quad (15.b)$$

.....

$$E_n = E_{0n} + \frac{RT}{F}\ln\frac{[Pol^{n+}(A^{-})_n]}{[Pol^{(n-1)+}(A^{-})_{n-1}][A^{-}]} \quad (15.c)$$

The concentration of any intermediate oxidation state can be expressed as a function of the concentration of the reactants (ions in solution and active centers in the film), the standard potential for the first equilibrium, and the potential steps for the consecutive equilibriums.

For a galvanostatic oxidation between two different and well-defined oxidation states of the film the potential must go on from the initial reduced state through n consecutive anodic steps defined by the concomitant standard potentials of each of the consecutive steps. The initial state of the polymer film is attained by reduction under the same conditions every time, and then the anodic current starts to flow. The initial potential is considered the origin of the experiment and adjusted to zero. From there the potential evolution will be defined by an initial potential step (to positive potentials) due to the system resistances. Then the potentials will evolve following the consecutive n steps of one electron oxidation step per polymer chain. The initial potential for every step being defined as function of the reactants concentrations from eqs 15.a to 15.c.

The opposite is valid for galvanostatic reduction adjusting the initial potential of the oxidized state to zero and the potentials moving to negative values through n consecutive reduction steps during flow of the cathodic current. From eqs 12.a and 12.b, the potential E_n (at every intermediate, n, state) will be given by

$$E_{an}(t) = E_{0n} + \frac{RT}{(1-\alpha)F}\left\{\ln\left(\frac{i_a}{FV}\right) - d\ln[A^{-}] - e\ln\left([Pol^{*}]_{initial} - \frac{i_a t}{FV}\right) - \ln k_{a0}\right\} \quad (16.a)$$

$$E_{cn}(t) = E_{0n} + \frac{RT}{\alpha F}\left\{\ln\left(\frac{i_c}{FV}\right) - \frac{k_c}{k_a}d\ln[A^{-}] - \frac{k_c}{k_a}e\ln\left(\frac{i_c t}{FV}\right) - \ln k_{c0}\right\} \quad (16.b)$$

The time of current flow required to extract, or inject, one electron in every chain of the film (the time t per oxidation or reduction step) is calculated from the charge (Q) consumed during the film oxidation (or reduction), the number (n) of individual electron transfer per chain (number of oxidation or reduction steps) and the experimental current, i

$$\frac{Q}{n} = it \Rightarrow t = \frac{Q}{ni} \quad (17)$$

The initial potential for any intermediate step n will be the final potential reached during the previous step (E_{n-1}) plus an increment (ΔE), see text and Figure S1 from the Supporting Information. By assuming that this increment is constant between the different oxidation or reduction states (the different steps)

$$E_{0n} = E_{n-1} + \Delta E = E_{n-2} + \Delta E + \Delta E = E_{01} + (n-1)\Delta E \quad (18)$$

By including this term in eq 16

$$E_{an}(t) = E_0 + (n-1)\Delta E + \frac{RT}{(1-\alpha)F}\left\{\ln\left(\frac{i_a}{FV}\right) - d\ln[A^{-}] - e\ln\left([Pol^{*}]_{initial} - \frac{i_a t}{FV}\right) - \ln k_{a0}\right\} \quad (19.a)$$

$$E_{cn}(t) = E_0 + (n-1)\Delta E + \frac{RT}{\alpha F}\left\{\ln\left(\frac{i_c}{FV}\right) - \frac{k_c}{k_a}d\ln[A^{-}] - \frac{k_c}{k_a}e\ln\left(\frac{i_c t}{FV}\right) - \ln k_{c0}\right\} \quad (19.b)$$

The potential evolution during the film oxidation, or reduction, is a result of the consecutive potential steps to every oxidation, or reduction, state and the potential evolution along every state. This is a function of consecutive steps as a Heaviside's function[88]

$$u(t) = \begin{cases} 0, \text{ if } t < 0 \\ 1, \text{ if } t \geq 0 \end{cases} \quad (20)$$

dx.doi.org/10.1021/jp300290s | J. Phys. Chem. B 2012, 116, 5279−5290

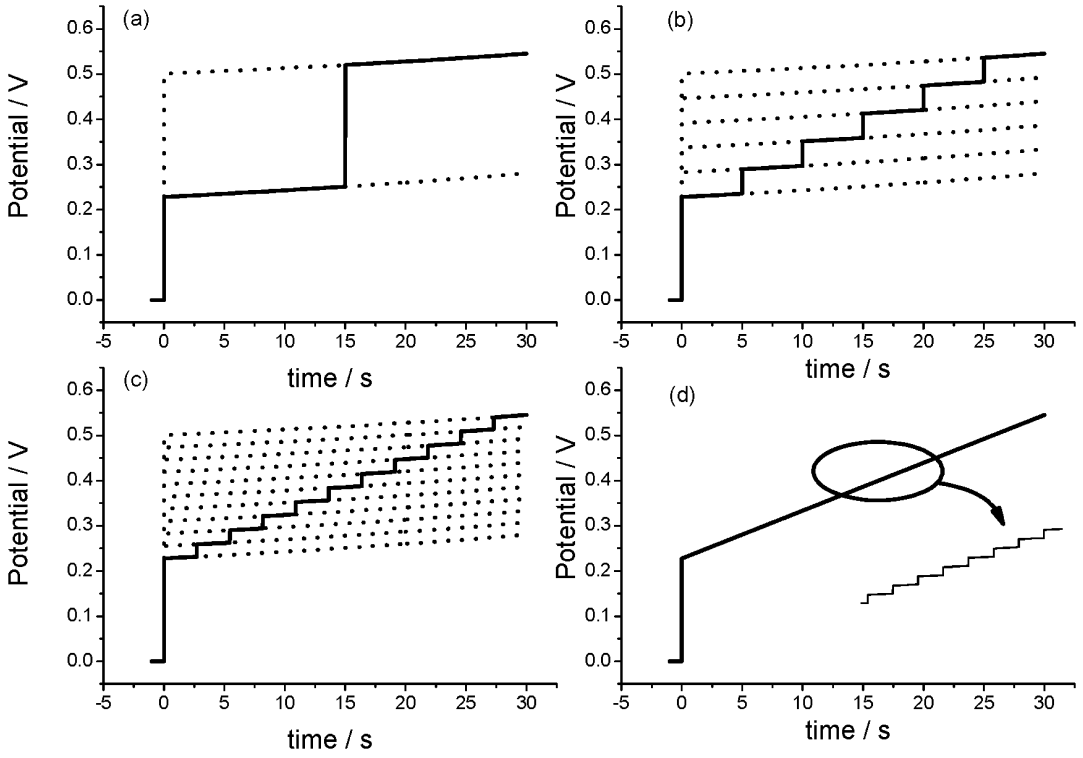

Figure 4. Simulated chronopotentiograms from eq 22 obtained for a different number (n) of intermediate oxidation states: (a) n = 2; (b) n = 6; (c) n = 11; (d) n = 3000. All the constants keep the same values stated for Figure 3.

From Heaviside's function it is possible to obtain the unitary pulse function, $p_n(t)$: $p_n(t)$ = 1 inside the time interval $[t_n, t_{n+1}]$, and $p_n(t)$ = 0 outside this time interval

$$p_n(t) = u(t - t_n) - u(t - t_{n+1}) = \begin{cases} 1, \text{ if } t \in [t_n, t_{n+1}] \\ 0, \text{ if } t \notin [t_n, t_{n+1}] \end{cases} \quad (21)$$

So, the potential evolution can be written as stair function, the result of consecutive unitary pulse functions

$$E(t) = \sum_{1}^{n} E_n(t)p_n(t) = E_1(t)p_1(t) + E_2(t)p_2(t) + \ldots + E_n(t)p_n(t) \quad (22)$$

Every $E_n(t)$ under flow of anodic currents is giving by eq 18.

Equation 22 was represented in Figure 4 (see also Figure S2 from the Supporting Information) for the same oxidation process (same Q) through different n stages: 2, 6, 11, or 3000 and for the same values of the constants above-defined for Figure 3.

For a high number of consecutive equilibrium steps (n) a constant slope is attained for the potential evolution. This faradic behavior used to be attributed in literature to a capacitive component of the electrochemistry of conducting polymers.[38−47]

At this point, it is worth mentioning that at the moment it is not possible to know either, how many polymer chains include a film of any electrogenerated conducting polymer, which their length distribution (polydispersity) is, or how many electrons can be removed from every polymeric chain through consecutive steps of one electron each. Thus, the number of electrons that can be removed from every polymeric chain has to be obtained by adjusting eq 22 to one of the experimental results, assuming that all the chains have the same length (monodisperse polymer), being the only adjustable magnitude of this theoretical development. Once adjusted the same value of n is used for the theoretical description at different temperatures.

This model also predicts the faster increase of the potential evolution, Figure 5, after oxidation completion of the active

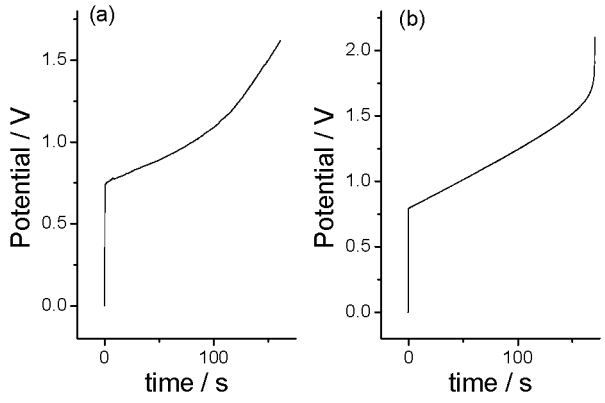

Figure 5. (a) Experimental chronopotentiograms obtained from a polypyrrole film when submitted to 0.4 mA in 0.1 M $LiClO_4$ aqueous solution having 1 cm^2 of the film inside the solution at room temperature (25 °C). (b) Simulation of eq 22 for n = 100, at room temperature (25 °C) passing a current of 0.4 mA, an initial concentration of active center, [*Pol**] = 0.7 mol L^{-1}; electrolyte concentration [A^-] = 1 M; assuming α = 0.5, for a polymeric film which *length* = 1 cm, *width* = 1 cm, *weight* = 1.6 mg, *density* = 1540 g L^{-1}.

dx.doi.org/10.1021/jp300290s | J. Phys. Chem. B 2012, 116, 5279−5290

centers in the polymer film, as expected after any oxidation (faradic) completion. Whether electrochemical responses from conducting polymers are capacitive or faradic remains a controversial aspect, outside the main scope of this paper, involving most of their electrochemical literature.[89,90]

Chronopotentiometric eqs 19.a and 19.b are the sensing functions of the reactive material, as self-supported electrode or as an electrode taking part of any electrochemical devices, for the following: temperature, mechanical conditions, electrolyte concentration, and current. We will focus now on the temperature influence by keeping a constant value for each of the other variables. Both equations can be simplified by including in one term all those taking constant values. The evolution of the potential for different temperatures (eq 19.a) becomes

$$E_a(t, T) = E_0 + (n-1)\Delta E + \frac{RT}{(1-\alpha)F}\left\{\ln\left(\frac{i_a}{FV}\right) - d\ln[A^-] - \ln k_{a0}\right\} - \frac{eRT}{(1-\alpha)F}\ln\left([Pol^*]_{initial} - \frac{i_a t}{FV}\right) = E_a(T) - E_a(t, T) \quad (23.a)$$

where

$$E_a(T) = E_0 + (n-1)\Delta E + \frac{RT}{(1-\alpha)F}\left\{\ln\left(\frac{i_a}{FV}\right) - d\ln[A^-] - \ln k_{a0}\right\} = \Delta E_{a0}(T) + (n-1)\Delta E \quad (24.a)$$

and

$$\Delta E_{a0}(T) = E_0 + \frac{RT}{(1-\alpha)F}\left\{\ln\left(\frac{i_a}{FV}\right) - d\ln[A^-] - \ln k_{a0}\right\} \quad (25.a)$$

Equation 25.a describes the potential step (ΔE_{a0}) at the beginning of the anodic current flow ($t \rightarrow 0$ s), as a linear function of the experimental temperature (T): the initial potential step senses the working temperature. The three terms inside the brackets result in a negative value: $\Delta E_{0a}(T)$ will take decreasing values for rising temperatures as will be demonstrated for the simulated results.

The second term from eq 23.a includes the potential evolution dependence on time of current flow and temperature

$$E_a(t, T) = -\frac{eRT}{(1-\alpha)F}\ln\left([Pol^*]_{initial} - \frac{i_a t}{FV}\right) \quad (26.a)$$

Equation 26.a is the temperature sensing function: the potential of conducting polymer films (self-supported or taking part of electrochemical devices) after a constant time of flow of an anodic current is a linear function of the experimental temperature. For rising times of current flow the second term in the parentheses increases, the parentheses decreases, and $E_a(t,T)$ decreases. So, the potential of the reacting film, $E_a(T) - E_a(t,T)$ increases with the time of current flow.

It is worth mentioning that for constant time experiments (same time implies same number of intermediate states), the potential has a linear relationship with temperature

$$E_{an}(t) = E_0 + (n-1)\Delta E + \frac{RT}{(1-\alpha)F}\left\{\ln\left(\frac{i_a}{FV}\right) - d\ln[A^-] - e\ln\left([Pol^*]_{initial} - \frac{i_a t}{FV}\right) - \ln k_{a0}\right\} = K_{a1} + TK_{a2} \quad (27.a)$$

where $K_{a1} = E_0 + (n-1)\Delta E$ and $K_{a2} = (R)/(1-\alpha)\{\ln((i_a)/(FV)) - d\ln[A^-] - e\ln([Pol^*]_{initial} - (i_a t)/(FV)) - \ln k_{a0}\}$ are both constants for a constant time.

Following a similar procedure, under flow of a constant cathodic current, i_c, starting from the oxidized material the potential evolution with time becomes

$$E_c(t, T) = E_0 + (n-1)\Delta E + \frac{RT}{\alpha F}\left\{\ln\left(\frac{i_c}{FV}\right) + \frac{k_c}{k_a}d\ln[A^-] - \ln k_{c0}\right\} + \frac{eRT}{\alpha F}\frac{k_c}{k_a}\ln\left(\frac{i_c t}{FV}\right) = E_c(T) + E_c(t, T) \quad (23.b)$$

where both ΔE and current take negative values

$$E_c(T) = E_0 + (n-1)\Delta E + \frac{RT}{\alpha F}\left\{\ln\left(\frac{i_c}{FV}\right) + \frac{k_c}{k_a}d\ln[A^-] - \ln k_{c0}\right\} = \Delta E_{c0}(T) + (n-1)\Delta E \quad (24.b)$$

and

$$\Delta E_{c0}(T) = E_0 + \frac{RT}{\alpha F}\left\{\ln\left(\frac{i_c}{FV}\right) + \frac{k_c}{k_a}d\ln[A^-] - \ln k_{c0}\right\} \quad (25.b)$$

This equation represents the potential step at the beginning of the current flow: is a linear function of the experimental temperature. The bracket takes a positive value giving decreasing negative values of $\Delta E_{c0}(T)$ for rising temperatures.

The second term is

$$E_c(t, T) = \frac{k_c}{k_a}\frac{eRT}{\alpha F}\ln\left(\frac{i_c t}{FV}\right) \quad (26.b)$$

Equation 26.b is the temperature sensing function: the potential of conducting polymer films (self-supported or taking part of electrochemical devices) after a constant time (t) of flow of a cathodic current is a linear function of the experimental temperature (T).

It is worth mentioning that for constant time experiments (same time implies same number of intermediate states), the potential has a linear relationship with temperature

$$E_{cn}(t) = E_0 + (n-1)\Delta E + \frac{RT}{\alpha F}\left\{\ln\left(\frac{i_c}{FV}\right) - \frac{k_c}{k_a}d\ln[A^-] - \frac{k_c}{k_a}e\ln\left(\frac{i_c t}{FV}\right) - \ln k_{c0}\right\} = K_{c1} + TK_{c2} \quad (27.b)$$

dx.doi.org/10.1021/jp300290s | J. Phys. Chem. B 2012, 116, 5279−5290

where $K_{c1} = E_0 + (n - 1)\Delta E$ and $K_{c2} = (R)/(\alpha F)\{\ln((i_c)/(FV)) - (k_c)/(k_a)d \ln[A^-](k_c)/(k_a)\ e \ln((i_c)/(FV)) - \ln k_{c0}\}$ are both constants for a constant time.

As a partial conclusion both, the initial potential step and the potential evolution with time inside every oxidation, or reduction, step are sensing linear functions of the experimental temperature.

Equations 23.a and 23.b have been simulated (Figure 6) for different temperatures (5, 10, 15, 20, and 25 °C); for n = 50; by flow of ±0.75 mA; being the initial specific concentration of active centers $[Pol^*]$ = 2 mol L^{-1}; the concentration of anions is solution $[A^-]$ = 1 M; assuming α = 0.5; for a polymeric film which *length* = 1 cm, *width* = 0.5 cm, *weight* = 1.6 mg; being the *film density* = 1540 g L^{-1}[191] and compared with experimental results. Experimental chronopotentiograms at different temperatures and under constant: anodic or cathodic current, electrolyte concentration, and concentration of the active centers in the film are also presented in Figure 6. A good agreement exists between theoretical and experimental results.

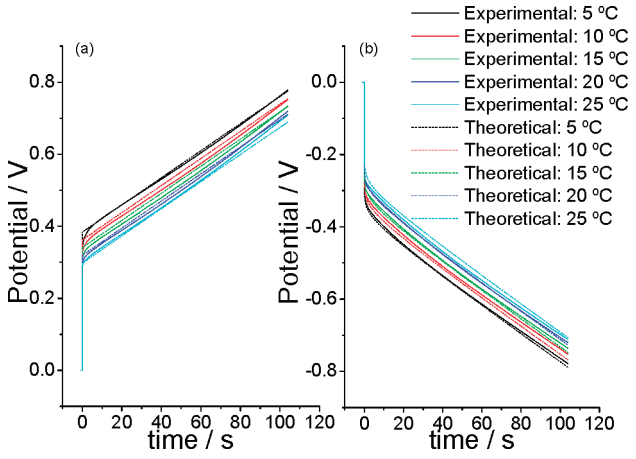

Figure 6. Chronopotentiograms obtained passing 0.75 mA (a) or −0.75 mA (b) through a polypyrrole film (10.77 mm × 5.09 mm × 19 μm) which mass after reduction is 1.6 mg at different temperatures (they are indicated in the figure) in 1 M $LiClO_4$ aqueous solution. In the figure the experimental chronopotentiogram (straight line) and the simulated chronopotentiogram from eq 22 (dotted line) are shown for different temperatures (5, 10, 15, 20, and 25 °C). Simulation constants: for n = 50; by flow of ±0.75 mA; being the initial concentration of active centers $[Pol^*]$ = 2 mol L^{-1}; electrolyte concentration $[A^-]$ = 1 M, assuming α = 0.5; for a polymeric film which *length* = 1 cm, *width* = 0.5 cm, *polypyrrole mass* = 1.6 mg; being the *film density* = 1540 g L^{-1}.

Either, the sensing stair function 22 describing the chronopotentiometric response and the sensing functions, 23.a and 23.b, defining the potential evolution inside the same oxidation step, describe and overlap the empirical results. They predict that after a constant time of current flow, that means when the material goes on through the same oxidation state, its potential results a linear function of the experimental temperature: the potential senses the actual temperature of the system. Under flow of a constant anodic or cathodic current of ±0.75 mA theoretical and experimental potentials after: 0 s (eqs 25.a and 25.b) or 30, 60 and 90 s (eqs 23.a and 23.b) are presented in Figure 7 having correlation coefficients (r^2), for the empirical

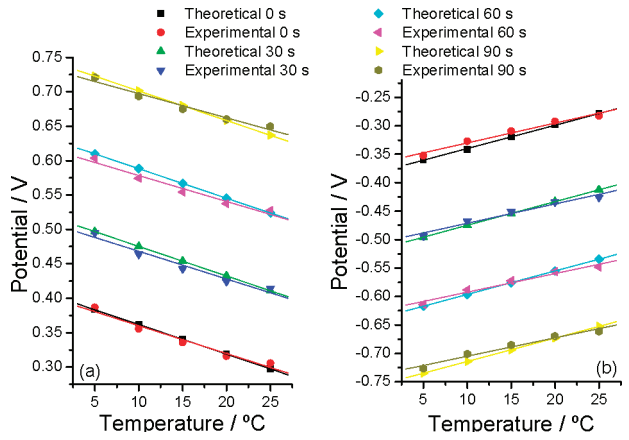

Figure 7. Evolution of the material potential with temperature obtained from Figure 6 after different times (0, 30, 60, and 90 s) of anodic (a) or cathodic (b) current flow. Theoretical representation for the temperature sensing functions, eq 25 (t = 0 s) and eq 23 (for the other times). Correlation coefficients for the experimental results are higher than 0.97.

results, higher than 0.97. Experimental and predicted slopes are very close corroborating the good theoretical description of the experimental results. Decreasing potentials at increasing temperatures, as expected from the Arrhenius expression for the chemical reaction constant, were obtained. Parallel linear variations were attained for different times of current flow: the temperature sensitivity (−4.05 mV K^{-1} for the oxidation and 3.71 mV K^{-1} for the reduction, average values) does not change with the reaction (oxidation or reduction) progress.

The electrical energy (U) consumed during the above oxidation or reduction processes is defined by

$$U_a(t) = i_a \int E_a(t)dt \tag{28.a}$$

where U_a is the consumed electrical energy during oxidation, i_a is the applied anodic current, and $E_a(t)$ is given by eq 23.a. Taking into account the two terms of this equation

$$\begin{aligned} U_a(t) &= i_a \int E_a(t)dt \\ &= i_a t\{E_0 + (n-1)\Delta E\} + \frac{RTi_a t}{(1-\alpha)F} \\ &\quad \left\{\ln\left(\frac{i_a}{FV}\right) - d\ln[A^-] - \ln k_{a0}\right\} + \frac{RTVe}{(1-\alpha)} \\ &\quad \left\{\ln\left([Pol^*]_{initial} - \frac{i_a t}{FV}\right) - 1\right\}\left\{[Pol^*] - \frac{i_a t}{FV}\right\} \\ &= tU_{a1} + TU_{a2}(t) \end{aligned} \tag{29.a}$$

And:

$$U_a(t) = tU_{a1} + TU_{a2}(t) \tag{30.a}$$

where U_{a1}

$$U_{a1} = i_a\{E_0 + (n-1)\Delta E\} \tag{31.a}$$

represents the constant energy per unit of time (U_a/t) consumed by the constant resistances of the system.

dx.doi.org/10.1021/jp300290s | J. Phys. Chem. B 2012, 116, 5279−5290

The second term TU_{a2} includes two components, the linear sensing function of consumed electrical energy with temperature (T) and a time dependent function $U_{a2}(t)$

$$U_{a2}(t) = \frac{Ri_a t}{(1-\alpha)F}\left\{\ln\left(\frac{i_a}{FV}\right) - d\ln[A^-] - \ln k_{a0}\right\} + \frac{RVe}{(1-\alpha)}\left\{\ln\left([Pol^*] - \frac{i_a t}{FV}\right) - 1\right\}\left\{[Pol^*] - \frac{i_a t}{FV}\right\} \quad (32.a)$$

Working at different temperatures all the terms but time are constant.

As a partial conclusion, eq 30.a states that the consumed electrical energy during the electrochemical oxidation of a conducting polymer film (as self-supported electrode or taking part of an electrochemical device) is a linear function of the experimental temperature: the consumed electrical energy, during oxidation, senses, at any time, temperature and temperature variations.

During reduction by flow of a constant cathodic current (i_c)

$$U_c(t) = i_c\int E_c(t)dt = i_c t\{E_0 + (n-1)\} + \frac{i_c tRT}{\alpha F}\left\{\ln\left(\frac{i_c}{FV}\right) + \frac{k_c}{k_d}d\ln[A^-] - \ln k_{c0} + \frac{k_c}{k_d}e\ln\left(\frac{i_c t}{FV}\right) - \frac{k_c}{k_d}e\right\} = tU_{c1} + TU_{c2}(t) \quad (29.b)$$

or

$$U_c(t) = tU_{c1} + TU_{c2}(t) \quad (30.b)$$

That includes the linear dependence of the consumed electrical energy with temperature, $T\,U_{c2}(t)$, and a time dependent function, $t\,U_{c1}$.

Being

$$U_{c1} = i_c\{E_0 + (n-1)\Delta E\} \quad (31.b)$$

the constant energy per unit of time (U_c/t) consumed by the different constant resistances of the system, and

$$U_{c2}(t) = \frac{i_c tR}{\alpha F}\left\{\ln\frac{i_c}{FV} + \frac{k_c}{k_a}d\ln[A^-] - \ln k_{c0} + \frac{k_c}{k_a}e\ln\left(\frac{i_c t}{FV}\right) - \frac{k_c}{k_a}e\right\} \quad (32.b)$$

Equation 30.b states that the consumed electrical energy during the electrochemical reduction of a conducting polymer film (as self-supported electrode or taking part of an electrochemical device) is a linear function of the experimental temperature: the consumed electrical energy, during reduction, senses, at any time, temperature and temperature variations.

Equations 29.a and 29.b were represented in Figure 8 for different experimental temperatures (5, 10, 15, 20, and 25 °C); under similar conditions that those above-defined for the potential evolution. Experimental results obtained by integration of the chronopotentiograms from Figure 6 also were overlapped in Figure 7.

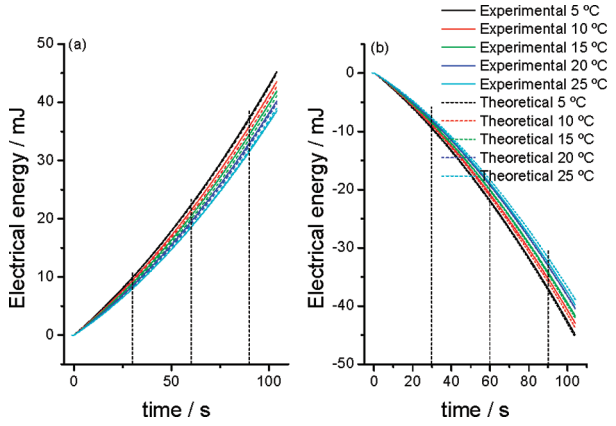

Figure 8. Evolution of the experimental consumed electrical energy along the reaction time at different temperatures (straight lines) by flow of the anodic (a) or cathodic (b) currents obtained by integration of the experimental chronopotentiograms shown in Figure 6. Theoretical evolution obtained by representation of eqs 30.a and 30.b (dotted lines).

Experimental and theoretical energies after different times of current flow: 30, 60, and 90 s are shown in Figure 9 for the

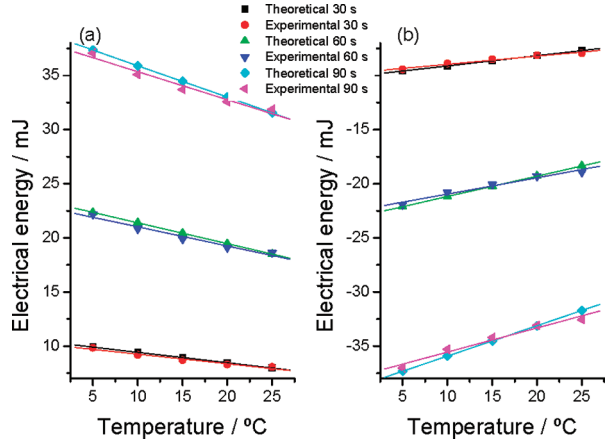

Figure 9. Electrical energy consumed to oxidize (a) or reduce (b) the polymer film after different times (30, 60, and 90 s) of current (anodic or cathodic, respectively) flowing at different temperatures. The experimental points were taken from Figure 8. Theoretical points were obtained from eq 30.a and 30.b for the anodic or cathodic processes, respectively. Higher correlation coefficients than 0.98 were obtained from the experimental results.

different studied temperatures. The correlation coefficients from the experimental results were higher than 0.98, corroborating the good linear dependence. At higher temperatures more thermal energy is available, and the reaction 1 consumes a lower electrochemical energy so the material potential is lower (eq 4.a). The obtained lines are not parallel because in eqs 32.a and 32.b, $U_{a2}(T)$ and $U_{c2}(T)$ are not linear functions of t. The system is most sensitive, presents higher slopes, for higher consumed energies, which means for a higher number of electrons extracted from every chain. Whatever the oxidation state experimental and theoretical results overlap corroborating the good theoretical description. Figure S3 from the Supporting Information shows the good agreement between empirical and theoretical slope variations as linear functions of the oxidation time (oxidation state).

dx.doi.org/10.1021/jp300290s | J. Phys. Chem. B 2012, 116, 5279−5290

Experimental results from Figure 6 are similar to those obtained at different temperatures from bending bilayer[79] or triple layer[33,35,86] artificial muscles, exchanging anions[33,35,79] or cations[86] with the electrolyte while describing the same angular movement (moving between the same initial and final oxidation states). The sensing eqs 19, 22 or 30 include the driving current and the potential or energy evolution. The driving current and the driving charge control the rate of the angular movement, the described angle and the new position of the muscle after movement.[11,35,37] So, eqs 19, 22 or 30 quantify simultaneously both, sensing and actuating properties of the device: they are dual actuating-sensing equations. The driving current (responsible for the mechanical actuation) and the sensing signal (the material or the device potential) are simultaneously present in the two connecting wires. The computer reads, at any time, during the movement of the muscle both, mechanical magnitudes (movement rate, direction, described angle and position) through the time of current flow (applied current and charge), and the working conditions (the working temperature here) through the potential or the consumed energy. The sensing eqs 19 and 30 explain empirical results previously obtained from the different studied artificial muscles.[33,34,79,86]

Being eqs 19, 22 or 30 related to the electrochemistry of conducting polymers any device: artificial muscle, battery, smart window or smart mirror, smart membrane or drug delivery systems based on the electrochemistry of conducting polymers will sense, while working by change of the oxidation state, temperature and ambient conditions, as artificial muscles do.

For real polydisperse materials iterative descriptions are required treating the influence of the different chain lengths on their first, second...n^{th} oxidation potential (Hückel approach) and on the number of oxidation steps per chain. The oxidation starts by extracting electrons from the longer chains. Only the shorter chains, requiring higher oxidation potentials according with Hückel rules, remain partially oxidized at the end of the oxidation completion. These laborious and space consuming mathematical treatments do not provide extra conceptual clarifications.

In subsequent papers we will develop those dual sensing-actuating equations for muscles, batteries, or devices sensing the ionic concentration in the liquid or solid electrolyte or sensing the mechanical conditions of work.

CONCLUSIONS

A theoretical description of chronopotentiometric responses from conducting polymer films (as self-supported electrodes or taking part of electrochemical devices) submitted to galvanostatic control as a function of the experimental variables has been attained. The model was developed from basic concepts of thermodynamics and electrochemical kinetics. Only reversible slow redox processes taking place in the polymer film are described. The process is assumed to occur under chemical kinetic control. Conformational relaxation kinetic control, or counterion diffusion kinetic control, was avoided in this initial approach. Irreversible parallel processes, as overoxidation or degradation reactions or electrolyte discharge, were not included in this stage of the theoretical development.

By assuming one electron transfer per polymer chain the simulated chronopotentiogram describes and quantifies the influence of the experimental variables: temperature, electrolyte concentration, or current on the shift of the chronopotentiometric (sensing property) responses. Nevertheless, the attained flat battery-like evolution of the potential is far from the high experimental chronopotentiometric slope.

In a second approach a monodisperse polymer film was considered, every chain losing n electrons during oxidation by flow of a constant anodic or cathodic current through n consecutive oxidation steps of one electron per step. By assuming that the potential step between two neighbor states is constant a good theoretical description of the experimental chronoamperograms is attained.

Under those conditions the theoretical equation predicts a high slope for the chronopotentiograms overlapping experimental results. The attained stair equations constitute the theoretical support for the faradic origin of those high slopes.

The theoretical stair function describes a fast increase of the material potential after oxidation completion, once the active centers were consumed, in good agreement with experimental results and with its faradic origin.

Every attained theoretical function describes the potential evolution during oxidation or reduction of films (as self-supported electrode or taking part of electrochemical devices) as a function of the following: the time of current flow, the concentration of the electrolyte, the working temperature, the film volume, or the experimental current. Those are multisensing functions.

The theoretical function predicts that, whatever the working temperature, the film potential (as self-supported electrode or taking part of an electrochemical device) after a constant time of current flow is a linear function of the experimental temperature: the actual potential of the material while reacting senses the working temperature. By changing temperature and keeping constant values of the other variables, a good agreement was attained between simulated and experimental chronopotentiograms.

The consumed electrical energy, obtained by integration of the chronopotentiogram, between two defined oxidation states of any conducting polymers is a sensing function of the experimental variables (temperature, electrolyte concentration, current, and so on). The energy sensing equation fits experimental results for different temperatures using polypyrrole films.

The attained theoretical equations allow describing the experimental chronopotentiograms from bilayer or triple-layer artificial muscles from the literature. The linear empirical variation of the muscle potential, or of their consumed electrical energies, with temperature, also becomes clarified now for muscles constituted by polymers films exchanging anions or for those constituted by polymer films exchanging cations with the electrolyte.

The attained equations are dual sensing-actuating functions. Actuating (current) and sensing (potential) magnitudes are present, at any time, by the two connecting wires, mimicking brain-organs communication. The reactive conducting polymers behave, simultaneously, as actuator and as sensors opening a new technological paradigm: several devices (one actuator and several sensors) in one under perfect and simultaneous control of sensing and actuating magnitudes.

Being general equations for the electrochemistry of conducting polymers, any electrochemical device (artificial muscle, battery, smart window, smart mirror, smart membrane, drug delivery, and so on) will sense working conditions. All of them will behave as dual and simultaneous acting-sensing devices.

■ ASSOCIATED CONTENT

Supporting Information

Mathematical development and simulation considering n equivalent oxidation steps; changes in the temperature sensitivity with the experimental reaction time are presented. This material is available free of charge via the Internet at http://pubs.acs.org.

■ AUTHOR INFORMATION

Corresponding Author

*Phone: +34 968 325519. Fax: +34 968 325915. E-mail: toribio.fotero@upct.es.

Notes

The authors declare no competing financial interest.

■ ACKNOWLEDGMENTS

The authors acknowledge financial support from Spanish Government (MCI) Projects MAT2008-06702 and Seneca Foundation Project 08684/PI/08. Jose G. Martinez acknowledges Spanish Education Ministry for a FPU grant (AP2010-3460).

■ REFERENCES

(1) Conzuelo, L. V.; Arias-Pardilla, J.; Cauich-Rodriguez, J. V.; Smit, M. A.; Otero, T. F. *Sensors* **2010**, *10*, 2638−2674.
(2) Bockris, J. O.; White, R. E.; Conway, B. E., Eds.; *Modern Aspects of Electrochemistry*; Kluwer Academic, Plenum Publishers: New York, 1999.
(3) Otero, T. F.; Cortes, M. T. *Chem. Commun.* **2004**, 284−285.
(4) Otero, T. F.; Cortes, M. T. *Adv. Mater.* **2003**, *15*, 279−282.
(5) Skotheim, T. A.; Reynolds, J. R., Eds.; *Handbook of Conducting Polymers*; CRC Press: New York, 2006.
(6) Entezami, A. A.; Massoumi, B. *Iran. Polym. J.* **2006**, *15*, 13−30.
(7) Otero, T. F.; Sansinena, J. M. *Bioelectrochem. Bioenerg.* **1995**, *38*, 411−414.
(8) Mirfakhrai, T.; Madden, J. D. W.; Baughman, R. H. *Mater. Today* **2007**, *10*, 30−38.
(9) Smela, E. *Adv. Mater.* **2003**, *15*, 481−494.
(10) Jager, E. W. H.; Smela, E.; Inganas, O. *Science* **2000**, *290*, 1540−1545.
(11) Valero, L.; Arias-Pardilla, J.; Cauich-Rodriguez, J.; Smit, M. A.; Otero, T. F. *Electrochim. Acta* **2011**, *56*, 3721−3726.
(12) Padilla, J.; Otero, T. F. *Electrochem. Commun.* **2008**, *10*, 1−6.
(13) Seshadri, V.; Padilla, J.; Bircan, H.; Radmard, B.; Draper, R.; Wood, M.; Otero, T. F.; Sotzing, G. A. *Org. Electron.* **2007**, *8*, 367−381.
(14) Rosseinsky, D. R.; Mortimer, R. J. *Adv. Mater.* **2001**, *13*, 783−787.
(15) Stenger-Smith, J. D. *Prog. Polym. Sci.* **1998**, *23*, 57−79.
(16) Ariza, M. J.; Otero, T. F. *Colloids Surf., A* **2005**, *270*, 226−231.
(17) Iyoda, T.; Ohtani, A.; Shimidzu, T.; Honda, K. *Chem. Lett.* **1986**, 687−690.
(18) Ehrenbeck, C.; Juttner, K. *Electrochim. Acta* **1996**, *41*, 511−518.
(19) Pile, D. L.; Hillier, A. C. *J. Membr. Sci.* **2002**, *208*, 119−131.
(20) Pellegrino, J. *Ann. N.Y. Acad. Sci.* **2003**, *984*, 289−305.
(21) Partridge, A. C.; Milestone, C.; Too, C. O.; Wallace, G. G. *J. Membr. Sci.* **1997**, *132*, 245−253.
(22) Malinauskas, A.; Malinauskiene, J.; Ramanavicius, A. *Nanotechnology* **2005**, *16*, R51−R62.
(23) Pan, L. J.; Qiu, H.; Dou, C. M.; Li, Y.; Pu, L.; Xu, J. B.; Shi, Y. *Int. J. Mol. Sci.* **2010**, *11*, 2636−2657.
(24) Novak, P.; Muller, K.; Santhanam, K. S. V.; Haas, O. *Chem. Rev.* **1997**, *97*, 207−281.
(25) Killian, J. G.; Coffey, B. M.; Gao, F.; Poehler, T. O.; Searson, P. C. *J. Electrochem. Soc.* **1996**, *143*, 936−942.
(26) Zinger, B.; Miller, L. L. *J. Am. Chem. Soc.* **1984**, *106*, 6861−6863.
(27) Guiseppi-Elie, A. *Biomaterials* **2010**, *31*, 2701−2716.
(28) Schmidt, C. E.; Shastri, V. R.; Vacanti, J. P.; Langer, R. *Proc. Natl. Acad. Sci. U.S.A.* **1997**, *94*, 8948−8953.
(29) Kotov, N. A.; Winter, J. O.; Clements, I. P.; Jan, E.; Timko, B. P.; Campidelli, S.; Pathak, S.; Mazzatenta, A.; Lieber, C. M.; Prato, M.; et al. *Adv. Mater.* **2009**, *21*, 3970−4004.
(30) Sullivan, J. T.; Harrison, K. E.; Mizzell, J. P.; Kilbey, S. M. *Langmuir* **2000**, *16*, 9797−9803.
(31) Isaksson, J.; Tengstedt, C.; Fahlman, M.; Robinson, N.; Berggren, M. *Adv. Mater.* **2004**, *16*, 316−320.
(32) Aoki, K.; Cao, J.; Hoshino, Y. *Electrochim. Acta* **1994**, *39*, 2291−2297.
(33) Otero, T. F.; Cortes, M. T. *Sens. Actuators, B* **2003**, *96*, 152−156.
(34) Valero, L.; Arias-Pardilla, J.; Smit, M.; Cauich-Rodriguez, J.; Otero, T. F. *Polym. Int.* **2010**, *59*, 337−342.
(35) Otero, T. F.; Cortes, M. T.; Arenas, G. V. *Electrochim. Acta* **2007**, *53*, 1252−1258.
(36) Otero, T. F. *J. Mater. Chem.* **2009**, *19*, 681−689.
(37) Otero, T. F.; Sansinena, J. M. *Bioelectrochem. Bioenerg.* **1997**, *42*, 117−122.
(38) Cebeci, F. C.; Sezer, E.; Sarac, A. S. *Electrochim. Acta* **2009**, *54*, 6354−6360.
(39) Servagent, S.; Vieil, E. *Synth. Met.* **1989**, *31*, 127−139.
(40) Hu, C. C.; Chen, E.; Lin, J. Y. *Electrochim. Acta* **2002**, *47*, 2741−2749.
(41) Hu, C. C.; Li, W. Y.; Lin, J. Y. *J. Power Sources* **2004**, *137*, 152−157.
(42) Dione, G.; Dieng, M. M.; Aaron, J. J.; Cachet, H.; Cachet, C. *J. Power Sources* **2007**, *170*, 441−449.
(43) An, H.; Wang, Y.; Wang, X.; Zheng, L.; Wang, X.; Yi, L.; Bai, L.; Zhang, X. *J. Power Sources* **2010**, *195*, 6964−6969.
(44) Tripathi, S. K.; Kumar, A.; Hashmi, S. A. *Solid State Ionics* **2006**, *177*, 2979−2985.
(45) Hashmi, S. A.; Latham, R. J.; Linford, R. G.; Schlindwein, W. S. *Polym. Int.* **1998**, *47*, 28−33.
(46) Soudan, P.; Lucas, P.; Ho, H. A.; Jobin, D.; Breau, L.; Belanger, D. *J. Mater. Chem.* **2001**, *11*, 773−782.
(47) Wang, J.; Xu, Y.; Chen, X.; Du, X. *J. Power Sources* **2007**, *163*, 1120−1125.
(48) Otero, T. F.; Grande, H.; Rodriguez, J. *J. Phys. Chem. B* **1997**, *101*, 8525−8533.
(49) Otero, T. F.; Grande, H.; Rodriguez, J. *Synth. Met.* **1997**, *85*, 1077−1078.
(50) Cao, J.; Aoki, K. *Electrochim. Acta* **1996**, *41*, 1787−1792.
(51) Tanguy, J.; Mermilliod, N.; Hoclet, M. *Synth. Met.* **1987**, *18*, 7−12.
(52) Kaplin, D. A.; Qutubuddin, S. *J. Electrochem. Soc.* **1993**, *140*, 3185−3190.
(53) Vorotyntsev, M. A.; Vieil, E.; Heinze, J. *Electrochim. Acta* **1996**, *41*, 1913−1920.
(54) Otero, T. F.; Grande, H.; Rodriguez, J. *J. Electroanal. Chem.* **1995**, *394*, 211−216.
(55) Otero, T. F.; Grande, H. *J. Electroanal. Chem.* **1996**, *414*, 171−176.
(56) Otero, T. F.; Grande, H. J.; Rodriguez, J. *J. Phys. Chem. B* **1997**, *101*, 3688−3697.
(57) Yap, W. T.; Durst, R. A.; Blubaugh, E. A.; Blubaugh, D. D. *J. Electroanal. Chem.* **1983**, *144*, 69−75.
(58) Posey, F. A.; Morozumi, T. *J. Electrochem. Soc.* **1966**, *113*, 176−184.
(59) Hillman, A. R.; Bruckenstein, S. *J. Chem. Soc., Faraday Trans.* **1993**, *89*, 339−348.
(60) Randriamahazaka, H.; Plesse, C.; Teyssie, D.; Chevrot, C. *Electrochim. Acta* **2005**, *50*, 4222−4229.
(61) Bobacka, J.; Lewenstam, A.; Ivaska, A. *J. Electroanal. Chem.* **2001**, *509*, 27−30.
(62) Micka, K.; Rousar, I.; Papez, V. *Electrochim. Acta* **1990**, *35*, 467−471.

(63) Pernaut, J. M.; Soares, L. C.; Belchior, J. C. *J. Braz. Chem. Soc.* **1997**, *8*, 175−180.
(64) Otero, T. F.; Angulo, E.; Rodriguez, J.; Santamaria, C. *J. Electroanal. Chem.* **1992**, *341*, 369−375.
(65) Vetter, K. J. *Electrochemical Kinetics. Theoretical Aspects*; Academic Press Inc.: New York, 1967.
(66) Otero, T. F.; Santos, F. *Electrochim. Acta* **2008**, *53*, 3166−3174.
(67) Otero, T. F.; Abadias, R. *J. Electroanal. Chem.* **2008**, *618*, 39−44.
(68) Otero, T. F.; Marquez, M.; Suarez, I. J. *J. Phys. Chem. B* **2004**, *108*, 15429−15433.
(69) Otero, T. F.; Martinez, J. G. *J. Solid State Electrochem.* **2011**, *15*, 1169−1178.
(70) Suarez, I. J.; Otero, T. F.; Marquez, M. *J. Phys. Chem. B* **2005**, *109*, 1723−1729.
(71) Spinks, G. M.; Liu, L.; Wallace, G. G.; Zhou, D. *Adv. Funct. Mater.* **2002**, *12*, 437−440.
(72) Spinks, G. M.; Wallace, G. G.; Liu, L.; Zhou, D. *Macromol. Sy.* **2003**, *192*, 161−169.
(73) Spinks, G. M.; Campbell, T. E.; Wallace, G. G. *Smart Mater. Struct.* **2005**, *14*, 406−412.
(74) Berdichevsky, Y.; Lo, Y. H. *Adv. Mater.* **2006**, *18*, 122−125.
(75) He, X. M.; Li, C.; Chen, F. E.; Shi, G. Q. *Adv. Funct. Mater.* **2007**, *17*, 2911−2917.
(76) Pei, Q. B.; Inganas, O. *J. Phys. Chem.* **1992**, *96*, 10507−10514.
(77) Pei, Q. B.; Inganas, O. *J. Phys. Chem.* **1993**, *97*, 6034−6041.
(78) Pei, Q. B.; Inganas, O. *Solid State Ionics* **1993**, *60*, 161−166.
(79) Ismail, Y. A.; Martinez, J. G.; Al Harrasi, A. S.; Kim, S. J.; Otero, T. F. *Sens. Actuators, B* **2011**, *160*, 1180−1190.
(80) Hara, S.; Zama, T.; Takashima, W.; Kaneto, K. *J. Mater. Chem.* **2004**, *14*, 1516−1517.
(81) Hara, S.; Zama, T.; Takashima, W.; Kaneto, K. *Synth. Met.* **2005**, *149*, 199−201.
(82) Hara, S.; Zama, T.; Takashima, W.; Kaneto, K. *Smart Mater. Struct.* **2005**, *14*, 1501−1510.
(83) Hara, S.; Zama, T.; Tanaka, N.; Takashima, W.; Kaneto, K. *Chem. Lett.* **2005**, *34*, 784−785.
(84) Hara, S.; Zama, T.; Takashima, W.; Kaneto, K. *Synth. Met.* **2006**, *156*, 351−355.
(85) Hara, S.; Zama, T.; Sewa, S.; Takashima, W.; Kaneto, K. *Chem. Lett.* **2003**, *32*, 576−577.
(86) Garcia-Cordova, F.; Valero, L.; Ismail, Y. A.; Otero, T. F. *J. Mater. Chem.* **2011**, *21*, 17265−17272.
(87) Atkins, P. W.; Depaula, J. *Physical Chemistry*; W H Freeman & Co.: New York, 2001.
(88) Abramowitz, M.; Stegun, I. A., Eds.; *Handbook of Mathematical Functions with Formulas, Graphs, and Mathematical Tables*; Dover: New York, 1972.
(89) Cosnier, S.; Karyakin, A., Eds.; *Electropolymerization: Concepts, Materials and Applications*; Wiley-VCH: Weinheim, 2010.
(90) Heinze, J.; Frontana-Uribe, B. A.; Ludwigs, S. *Chem. Rev.* **2010**, *110*, 4724−4771.
(91) Aldissi, M., Ed.; *Intrinsically Conducting Polymers: An Emerging Technology*; Kluwer Academic Publishers: Dordrecht, 1992.